

# MVAM: Multi-View Attention Method for Fine-grained Image-Text Matching

Wanqing Cui<sup>1,2</sup>[0000-0001-5015-5252]<sup>†</sup>, Rui Cheng<sup>3</sup>[0009-0009-1530-190X]<sup>†</sup>,  
Jiafeng Guo<sup>1,2</sup>[0000-0002-9509-8674]<sup>\*</sup>, and Xueqi Cheng<sup>1,2</sup>[0000-0002-5201-8195]

<sup>1</sup> CAS Key Laboratory of Network Data Science and Technology,  
Institute of Computing Technology, Chinese Academy of Sciences, Beijing, China

<sup>2</sup> University of Chinese Academy of Sciences, Beijing, China  
{cuiwanqing18z, guojiafeng, cxq}@ict.ac.cn

<sup>3</sup> Alibaba Group, Beijing, China  
guanyu.cr@alibaba-inc.com

**Abstract.** Existing two-stream models, such as CLIP, encode images and text through independent representations, showing good performance while ensuring retrieval speed, have attracted attention from industry and academia. However, the single representation often struggles to capture complex content fully. Such models may ignore fine-grained information during matching, resulting in suboptimal retrieval results. To overcome this limitation and enhance the performance of two-stream models, we propose a **Multi-View Attention Method** (MVAM) for image-text matching. This approach leverages diverse attention heads with unique view codes to learn multiple representations for images and text, which are then concatenated for matching. We also incorporate a diversity objective to explicitly encourage attention heads to focus on distinct aspects of the input data, capturing complementary fine-grained details. This diversity enables the model to represent image-text pairs from multiple perspectives, ensuring a more comprehensive understanding and alignment of critical content. Our method allows models to encode images and text from different perspectives and focus on more critical details, leading to better matching performance. Our experiments on MSCOCO and Flickr30K demonstrate enhancements over existing models, and further case studies reveal that different attention heads can focus on distinct content, achieving more comprehensive representations.

**Keywords:** Image-text retrieval · Multi-representation learning · Multi-modal.

## 1 Introduction

Cross-modal image-text matching, recognized for its broad application prospects in fields like product search and information retrieval, is a key task in multi-modal understanding and has garnered significant attention. Generally speaking,

<sup>†</sup> These authors contributed equally to this work.

<sup>\*</sup> Corresponding author.

Queries	A kitchen with two windows and two metal sinks.	A selection of wooden kitchen tools on a counter.	White ornate seat in nicely decorated room with television.
CLIP			
MVAM-CLIP			

**Fig. 1.** Examples of retrieved images with CLIP and our model MVAM-CLIP. CLIP retrieved images ignore some important information of texts. MVAM-CLIP retrieved images are more consistent with the texts.

there are two typical architectures: single-stream and two-stream. Single-stream models[17, 24, 30, 3, 19] utilize a unified encoder with full self-attention to encode images and texts. Although such methods tend to attain higher accuracy, they suffer from low inference efficiency since each pair of possible candidates needs to be recomputed during inference, thus limiting the application in practical scenes. Two-stream models [8, 40, 16, 31, 12] employ separate self-attention mechanisms for images and texts, encoding inputs from each modality independently. These models combine the representations only at the final stage to compute matching scores, which enhances inference efficiency and makes them highly suitable for practical applications. In addition, models like CLIP [31] that have both efficiency and effectiveness are often used in various downstream tasks, such as image generation [32, 2, 36], image manipulation [28, 29, 15], semantic segmentation [22, 9, 41, 27] and so on.

However, two-stream models typically yield sub-optimal results due to their limited interaction between image and text modalities and inadequate comprehensive representation capabilities. They rely on a singular pre-encoded representation for images or text, which often fails to capture fine-grained information during retrieval, especially with complex inputs. As the example shown in Figure 1, even the advanced CLIP model, trained on a large-scale corpus, struggles to encode all required details. Given the query text "A kitchen with two windows and two metal sinks", CLIP overlooks "two windows" and returns an image that doesn't match exactly.

To enhance representation capabilities in two-stream models, in this paper, we introduce a novel **Multi-View Attention Model** (MVAM), which separately

represents images and texts in diverse views using distinct attention heads. Then these multi-view representations will be concatenated as the final representation for matching. We also introduce a diversity objective to promote diversity among different attention views and enrich the features. As demonstrated in Figure 1, by capturing detailed information comprehensively, MVAM successfully retrieves the most suitable images. As a pluggable method, MVAM can be seamlessly integrated with any two-stream model.

We conduct experiments on two popular datasets, i.e., MSCOCO [21] and Flickr30K [39]. Experimental results indicate a significant performance improvement over existing methods. Further analysis shows that different attention heads of MVAM do respond specifically to different details of images or text.

The contributions of this work can be concluded as the following: (1) We introduce a novel image-text matching method MVAM, which can enhance the representation of two-stream models and thus improve the image-text matching performance. (2) We introduce a diversity loss to promote diversity among attention heads. (3) We exhaustively quantify the capability of our method on two benchmarks under various settings. Additionally, we provide case studies to offer an intuitive understanding of our method.

## 2 Related work

### 2.1 Two-stream Image-text Matching method

Two-stream models for image-text matching are categorized based on their image encoder architectures. **Faster-RCNN based models** firstly use Faster-RCNN models [33, 1] to detect bounding boxes and visual features of objects in images, known as regional features. Then the text and image features are encoded through RNN and RCNN [13, 16, 37] or transformer [35, 11] to obtain the final representation. To achieve a fast retrieval speed, VisaulSparta [25] practices an inverted index on text-to-image search and caches the relevance of all candidate images and all words in vocabulary as the lookup table. **ViT based models** [7] firstly splits an image into multiple patches and use ViT [7] to encode image into visual patch representations. CLIP [31] and ALIGN [12] are the two most known ViT-based cross-modal matching models. They establish relations between image and text by training on large-scale unlabeled image-text pairs from the web. Among them, CLIP is an open-source model, which achieves excellent performance on multiple image-text matching tasks.

### 2.2 Multi-Representation Learning

Previous works on extracting key components from complex inputs primarily focus on text [23, 10, 26, 14], using multiple self-attention layers to encode instances into vectors. For visual inputs, SpaAttn [18] uses spatial attention to represent images as multi-vectors, enhancing person re-identification. As for improving the quality of representation used for cross-modal matching, MVPTR [20] constructs

multi-level semantics for both language and vision inputs. PVSE [34] is the most related to our work. It encodes polysemous instances using  $k$  embeddings and selects the maximum similarity score from all combinations. However, this approach might ignore mismatches since it focuses solely on the most compatible aspect. Additionally, calculating each combination results in high computational costs and can hinder the model’s convergence. In contrast, our model considers all views from different aspects during matching in a single calculation, improving both performance and efficiency.

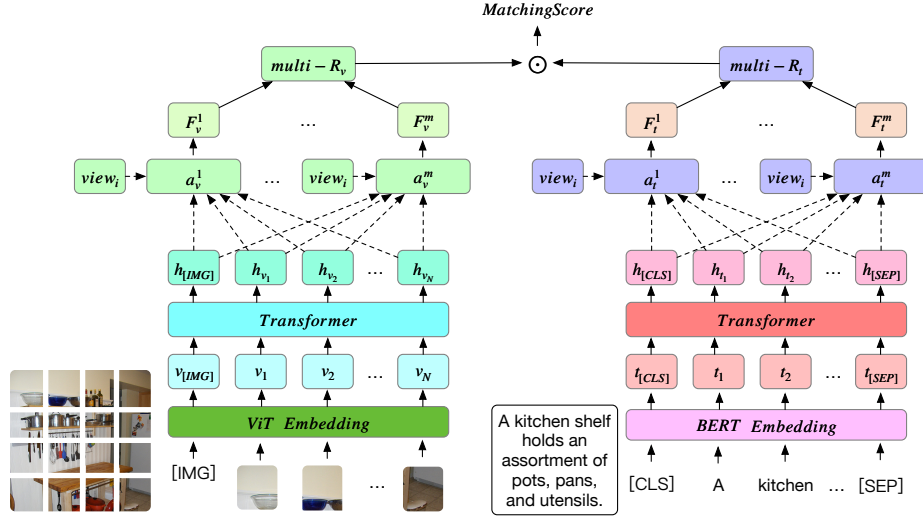


Fig. 2. The network architecture of MVAM with ViT encoder.

### 3 Method

All of our models are built on top of the two-stream matching model. Therefore, in this section, we first briefly review the architecture and training objective of two-stream models. To save space, we take the ViT-based structure as an example. Then we describe the details of the Multi-View Attention Method and the multi-view diversity loss.

#### 3.1 Two-stream Image-text Matching Model

**Image Encoder** Given an input image  $V \in \mathbb{R}^{H \times W \times C}$ , where  $(H, W)$  is the resolution of the image and  $C$  is the number of channels, we first split it into a sequence of flattened 2D patches  $V_p \in \mathbb{R}^{N \times (P^2 C)}$ , in which  $N = HW/P^2$



is the number of patches and  $(P, P)$  is the resolution. To get contextual representations, a special token  $[IMG]$  is also prepended to the patches. Then we use a ViT model [7] to encode the patches and get their hidden states  $H_v = \{h_{[IMG]}, h_{v_1}, \dots, h_{v_N}\}$ . The final image representation is the pooling of the hidden states of  $[IMG]$  token:

$$H_v = Transformer([IMG]; V_p), \quad (1)$$

$$R_v = Pool(h_{[IMG]}). \quad (2)$$

**Text Encoder** An input sentence  $T$  is firstly split into a sequence of tokens  $\{[CLS], t_1, \dots, t_L, [SEP]\}$ , in which  $[CLS]$  and  $[SEP]$  are special tokens that mark start and end. Then we use BERT [5] to encode the inputs into  $L + 2$  hidden states  $H_t = \{h_{[CLS]}, h_{t_1}, \dots, h_{t_L}, h_{[SEP]}\}$  and get the text representation  $R_t$  by pooling the hidden states of  $[CLS]$  token.

$$H_t = Transformer([CLS]; T; [SEP]), \quad (3)$$

$$R_t = Pool(h_{[CLS]}). \quad (4)$$

### 3.2 Training Objective

Following CLIP [31] and LightningDOT [35], The matching score is the cosine similarity between the image representation and the text representation. We use the in-batch contrastive loss as the learning objective, which consists of an image-to-text retrieval loss  $loss_{i2t}$  and a text-to-image loss  $loss_{t2i}$ . Specifically, given a batch of  $B \times B$  image-text pairs, the loss of image-to-text retrieval is:

$$loss_{i2t} = -\frac{1}{B} \sum_{i=1}^B \log \frac{e^{\cos(R_{v_i}, R_{t_i})}}{\sum_{j=1}^B e^{\cos((R_{v_i}, R_{t_j}))}}, \quad (5)$$

Similarly, we calculate the text-to-image retrieval loss  $loss_{t2i}$  and the final contrastive loss is:

$$loss_{cl} = \frac{1}{2}(loss_{i2t} + loss_{t2i}). \quad (6)$$

### 3.3 Encode with Multi-View Attention Method (MVAM)

To enhance the representation capabilities of two-stream matching models and encode more information, we introduce the Multi-View Attention Method (MVAM). The architecture of MVAM with ViT encoder is shown in Figure 2. After encoding an image or a text into hidden states with encoder, instead of using a pooled hidden state as representation, MVAM obtains the multi-viewed representations through multi-attention heads, results in multiple vectors for one instance.

Take the image as an example. To obtain diverse visual representations,  $m$  learnable view codes  $(c_v^1, \dots, c_v^m)$  are used as the queries to guide attention, where

$c_v^i \in \mathbb{R}^D$  and  $D$  is the dimension of  $h_{v_i}$ . Therefore, we can get  $m$  diverse view features  $(F_v^1, \dots, F_v^m)$  of an input image from  $m$  perspective:

$$a_v^i = \text{softmax}(H_v * c_v^i), \quad (7)$$

$$F_v^i = \sum_{j=0}^N a_v^{(i,j)} * H_v^j. \quad (8)$$

The final representation of an image  $R_v^*$  is the concatenation of  $m$  diverse view features:

$$R_v^* = [F_v^1; F_v^2; \dots; F_v^m]. \quad (9)$$

Similarly, we can also get the multi-view representation  $R_t^*$  of text.

### 3.4 Multi-View Diversity Loss

To further enrich the diversity of features from different views and enable comprehensive information encoding, we implement a diversity loss to accentuate differences between the multi-view attention weights [18, 23]. This ensures that the multi-view codes can highlight various aspects of an image or text.

For instance, consider an image represented through our model. We calculate the similarity among each view's attention weights  $A_v$ , which consists of  $[a_v^1, \dots, a_v^m]$ , by multiplying  $A_v$  by its transpose. We then subtract an identity matrix from this product, using the result as a measure of diversity. The diversity grows as the decrease of non-diagonal values of the similarity matrix, and a diversity loss  $loss_{div}^v$  is:

$$loss_{div}^v = \| (A_v A_v^T - I) \|_F^2, \quad (10)$$

where  $I$  is a  $m$ -dimensional identity matrix, which is used to remove the  $m$  view attention's self-correspondences on the diagonal of the similarity matrix.  $\| \cdot \|_F$  stands for the Frobenius norm of a matrix.

We also considered a variant, i.e. the square root diversity loss, which allows more large salient regions from a higher level. The loss function is as follows, in which  $E = \sqrt{A_v}$ :

$$loss_{div}^{v'} = \| (E_v E_v^T - I) \|_F^2 \quad (11)$$

We apply the same similar operation to text multi-view attention and obtain  $loss_{div}^t$ . The final loss is the sum of diversity loss, scaled by a coefficient  $\beta$ , and the contrastive loss:

$$loss_{div} = loss_{div}^v + loss_{div}^t, \quad (12)$$

$$loss = loss_{cl} + \beta(loss_{div}), \quad (13)$$

## 4 Experiments

### 4.1 Datasets

We evaluate the effectiveness of our proposed MVAM using MSCOCO[21]<sup>4</sup> and Flickr30K[39]<sup>5</sup> datasets, in which each image has 5 captions. The experimental task is image-text retrieval, which includes two subtasks: image-to-text retrieval (i2t), where an image is used as the query to retrieve relevant text descriptions, and text-to-image retrieval (t2i), where a text query is used to retrieve relevant images. Following the previous study [13], the MSCOCO dataset is divided into 114k/5k/5k for training, validation, and testing. We report results on both 1K unique test images (averaged over 5 folds) and the full 5K test images. The Flickr30K dataset is divided into 29K/1K/1K for training, validation, and testing.

For both datasets, the text queries are directly derived from the corresponding captions associated with the images. Each image is annotated with 5 human-written captions, which serve as queries for retrieval tasks. The ground truth for each query is established by associating each caption with its corresponding image. For each query, there is exactly one relevant image in the dataset. Conversely, in the image-to-text task, each image has 5 corresponding relevant text queries.

### 4.2 Metric

To evaluate the performance of our proposed MVAM model, we employ the Recall@K metric, which is commonly used in image-text retrieval tasks. Recall@K measures the proportion of ground-truth matches that are retrieved within the top-K results. A higher R@K indicates better retrieval performance. Specifically, we report results for i2t@K (image-to-text retrieval): given an image as the query, this metric evaluates how often the correct captions appear in the top-K retrieved text results, and t2i@K (text-to-image retrieval): given a text query, this metric evaluates how often the correct images appear in the top-K retrieved image results. These metrics are crucial because they directly reflect the system’s effectiveness in retrieving relevant items in practical scenarios, where returning the correct result within the top few ranks is essential for user satisfaction.

### 4.3 Baselines

We select **PVSE** [34], **SCAN** [16], **LightningDOT** [35] and **VisaulSparta** [25] from prior works as our baselines. We also implement 3 additional two-stream models based on 3 image encoders: FRCNN, ViT, and CLIP. Both models with FRCNN and ViT take the BERT<sub>base</sub> as the text encoder, which is initialized from bert-base-uncased [6], and the image encoder is a randomly initialized

<sup>4</sup> <https://cocodataset.org>

<sup>5</sup> <https://bryanplummer.com/Flickr30kEntities/>

transformer, which receives outputs from FRCNN and ViT [38, 4] as input respectively. The model with CLIP uses the same architecture as CLIP except for the final interaction module, and the parameters are initialized from the pre-trained CLIP(ViT-B/16) [31].

For a thorough comparison, we also try two ways to get the final representations of images and texts, i.e. [CLS] pooling (+[CLS]) and attention pooling (+Attn). The [CLS] pooling method utilizes a linear projection followed by a tanh function to map the [CLS] (or [IMG]) hidden states to a 1024-dimensional vector. Attention pooling first transforms the hidden states into 1024-dimensional vectors using a linear projection layer, and then aggregates these vectors using an attention head with only one view code.

#### 4.4 Implementation Details

We train models using a batch size of 1024 over 20 epochs. The learning rates of Base-FRCNN, Base-ViT, MVAM-FRCNN, and MVAM-ViT are  $5e-5$ . In Base-CLIP, the learning rate is set to  $5e-8$  for preserving the multi-modal alignment learned in CLIP. For MVAM-CLIP, We train it in 2 stages: firstly training view codes with the fixed CLIP model using  $5e-5$  learning rate, and secondly fine-tuning all parameters of MVAM-CLIP using  $5e-8$  learning rate. For all MVAM implementations, we design 16 view codes for images or texts. Coefficient  $\beta$  for diversity is set to 10. All experiments are run on  $8 \times$  NVIDIA V100 GPUs. The best development set accuracy from 3 random restarts is reported.

#### 4.5 Experiments Results

**Table 1.** Performance of all models on MSCOCO, with the highest scores bolded. The three blocks below represent the use of ViT, FRCNN, and CLIP as image encoders respectively. VS and LD stands for VisualSpart and LightningDOT.

Tasks		MSCOCO-1K						MSCOCO-5K					
	Recall	i2t@1	i2t@5	i2t@10	t2i@1	t2i@5	t2i@10	i2t@1	i2t@5	i2t@10	t2i@1	t2i@5	t2i@10
ViT	PVSE	69.2	91.6	96.6	55.2	86.5	93.7	45.2	74.3	84.5	32.4	63.0	75.0
	SCAN	72.7	94.8	98.4	58.8	88.4	94.8	50.4	82.2	90.0	38.6	69.3	80.4
	VS	-	-	-	68.7	91.2	96.2	-	-	-	45.1	73.0	82.5
	LD	-	-	-	-	-	-	60.1	85.1	91.8	45.8	74.6	83.8
	+ [CLS]	65.65	90.52	96.07	54.06	85.88	93.6	40.13	70.43	82.23	30.66	61.63	74.29
	+ Attn	65.79	90.62	95.87	55.12	86.44	93.83	41.56	70.67	81.61	32.59	62.9	75.24
	+ MVAM	70.02	92.09	96.75	56.69	87.35	94.46	46.6	75.33	84.64	33.54	64.53	76.46
	+ [CLS]	69.4	92.96	97.52	56.79	87.81	94.82	43.38	75.52	85.88	32.96	64.62	77.01
	+ Attn	72.3	93.92	97.7	58.53	88.22	94.74	47.46	77.66	87.34	35.25	66.48	78.02
	+ MVAM	77.0	95.34	98.28	62.11	90.04	95.64	54.08	82.46	90.06	39.08	69.94	80.92
FRCNN	+ [CLS]	69.4	92.96	97.52	56.79	87.81	94.82	43.38	75.52	85.88	32.96	64.62	77.01
	+ Attn	72.3	93.92	97.7	58.53	88.22	94.74	47.46	77.66	87.34	35.25	66.48	78.02
	+ MVAM	77.0	95.34	98.28	62.11	90.04	95.64	54.08	82.46	90.06	39.08	69.94	80.92
CLIP	+ [CLS]	80.86	96.08	98.44	67.54	91.74	96.5	62.93	85.32	91.66	47.49	74.81	84.06
	+ Attn	81.64	96.62	98.48	68.36	91.85	96.78	65.11	87.38	93.20	48.62	75.66	84.38
	+ MVAM	<b>83.14</b>	<b>97.04</b>	<b>99.02</b>	<b>69.35</b>	<b>92.33</b>	<b>97.12</b>	<b>66.81</b>	<b>88.3</b>	<b>93.88</b>	<b>49.47</b>	<b>76.48</b>	<b>84.9</b>

**Table 2.** Performance of all models on Flickr30K datasets.

	Recall	i2t@1	i2t@5	i2t@10	t2i@1	t2i@5	t2i@10
	SCAN	67.4	90.3	95.8	48.6	77.7	85.2
	VisualSparta	-	-	-	57.1	82.6	88.2
	LightningDOT	83.9	97.2	98.6	69.9	91.1	95.2
ViT	+ [CLS]	48.01	74.87	84.58	39.0	71.05	80.86
	+ Attn	55.2	83.0	89.9	43.66	73.96	83.16
	+ MVAM	55.57	82.53	90.09	44.54	75.04	84.49
FRCNN	+ [CLS]	51.2	78.4	86.3	39.98	71.36	81.32
	+ Attn	57.3	83.25	91.22	47.6	77.73	85.99
	+ MVAM	69.3	90.4	94.5	53.14	80.68	88.32
CLIP	+ [CLS]	89.6	98.3	<b>99.5</b>	76.32	93.88	96.54
	+ Attn	90.5	98.1	99.4	75.06	93.38	96.3
	+ MVAM	<b>91.8</b>	<b>98.7</b>	99.4	<b>76.44</b>	<b>94.22</b>	<b>97.16</b>

The results of all models on MSCOCO and Flickr30K are shown in Table 4.5 and Table 2. MVAM significantly enhances performance across various two-stream matching models. Notably, MVAM-CLIP outperforms competing methods such as PVSE, SCAN, LightningDOT, and VisualSparta, despite the latter two being pre-trained on more extensive multi-modal datasets with multiple learning objectives. When compared to ViT, FRCNN, and CLIP with attention pooling, MVAM shows increased average scores of 1.62%, 2.17%, and 0.71% on MSCOCO-1K, and 2.76%, 4.06%, 0.92% on MSCOCO-5K, respectively. On Flickr30K, the improvements are 0.56%, 5.54%, and 0.83%. Additionally, the greatest enhancements are observed with the FRCNN-based model, suggesting that MVAM is particularly effective with region-based image features. This may be due to the more comprehensive semantic information contained in region-based features, which better aligns with our method’s focus on critical points.

#### 4.6 More Analysis

In the subsequent paragraphs, we will discuss the results of our ablation studies and further analyze the MVAM. All experimental analyses are conducted using the FRCNN model on the MSCOCO dataset.

**The Effectiveness of Multi-view** To confirm that the performance enhancements are attributable to the adoption of multi-views and not merely the result of feature ensemble, we conduct specific ablation study. Specifically, in the ensemble setting, we employ 16 independent models with FRCNN, each generating a 64-dimensional representation vector through attention pooling. These vectors are then concatenated into a 1024-dimensional vector for image-text matching.

All 16 models shared the same network architecture but are initialized with randomly varied parameters using 16 different seeds during training. The results, presented in Table 3, clearly indicate that our method significantly outperforms the ensemble model. This confirms that the superior performance stems from the high-quality representations derived through multi-view attention, rather than from the ensemble technique.

**Table 3.** The comparisons of our model with ensemble methods on MSCOCO-5K.

ModelType	i2t@1	i2t@5	i2t@10	t2i@1	t2i@5	t2i@10
Base-FRCNN-ensemble	49.6	79.42	87.78	36.31	67.87	79.52
MVAM-FRCNN	<b>54.08</b>	<b>82.46</b>	<b>90.06</b>	<b>39.08</b>	<b>69.94</b>	<b>80.92</b>

**The Numbers of Views** We conduct extensive experiments to explore the impact of different numbers of view codes. The results, documented in Table 4, indicate a trend where matching accuracy initially increases with the number of views and then declines. Optimal performance was achieved with 16 views. We speculate that fewer views might ignore critical content thus failing to extract sufficient information for effective image-text matching. Conversely, an excessive number of views could introduce redundancy in the representations and lead to longer representation vectors, complicating the training process of the model.

**Table 4.** Ablation results of the number of views on MSCOCO-5K.

#Views	i2t@1	i2t@5	i2t@10	t2i@1	t2i@5	t2i@10
1	47.46	77.66	87.34	35.25	66.48	78.02
8	53.52	81.28	89.66	38.52	69.24	80.62
16	<b>54.08</b>	<b>82.46</b>	<b>90.06</b>	<b>39.08</b>	<b>69.94</b>	<b>80.92</b>
32	53.9	81.72	89.9	38.28	69.35	80.59

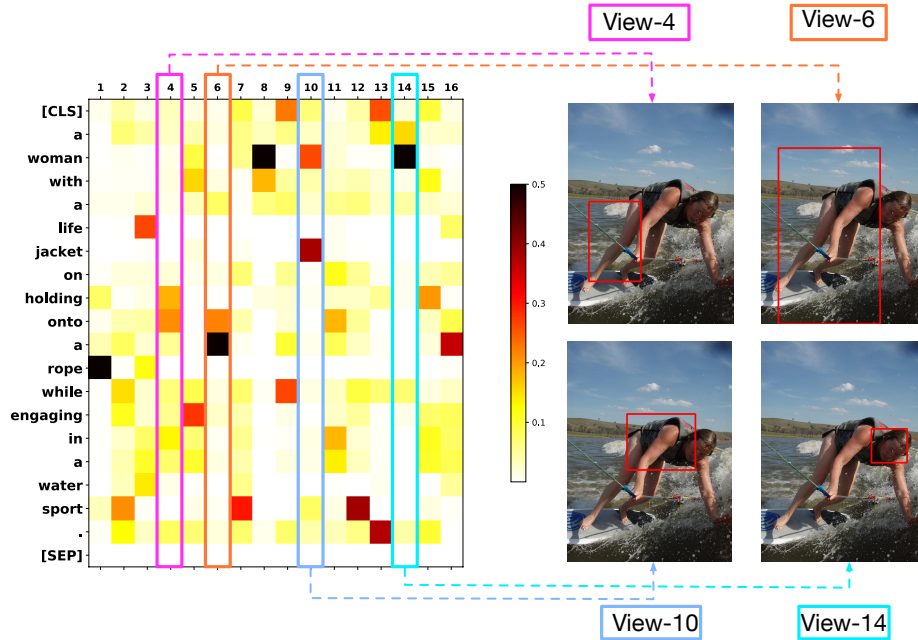
**Diversity Loss Analysis** The results of MVAM-FRCNN trained under three conditions, i.e. without diversity loss, with base diversity loss, and with square root diversity loss, are shown in Tabel 5. These results highlight the importance of multi-view diversity. The model performs best with base diversity loss. This may be due to the descriptive nature of texts in MSCOCO and Flickr30K, which makes it more effective to encourage the model to focus on isolated regions. For more abstract retrieval tasks, the square root diversity loss may be more beneficial, which needs further exploration in the future.

**Multi-view Interpretability** We visualize the attention maps to understand how our model interprets data from multiple views. As the example shown in

**Table 5.** Ablation results of diversity loss on MSCOCO-5K.

Diversity Loss	i2t@1	i2t@5	i2t@10	t2i@1	t2i@5	t2i@10
w/o diversity loss	54.06	81.98	90.04	38.64	69.65	80.74
square root diversity loss	<b>54.14</b>	82.44	<b>90.32</b>	38.82	69.8	80.73
base diversity loss	54.08	<b>82.46</b>	90.06	<b>39.08</b>	<b>69.94</b>	<b>80.92</b>








Figure 3, the attention from different views displays a sparse and diverse pattern, and each view concentrates on specific regions. This illustrates our method’s ability to encode images and texts from various aspect and highlight salient regions, thereby enriching the information contained in the representations. Further analysis reveals a one-to-one mapping relationship between the attention maps of image and text across different views. For instance, View-4 of the text concentrates on the phrase "holding onto," while View-4 of the image focuses on the area associated with "holding a rope." This illustrates that MVAM can comprehensively consider complex content and align multiple meanings cross modalities.



**Fig. 3.** The visualization of attention from different views. The left side provides the attention scores over text for all the 16 attention heads of MVAM, and the darker the grid color represents the greater the attention value. The right side shows the regions in the image that four of the view attention heads pay most attention to.

#### 4.7 Qualitative Case Analysis

Figure 4 shows the images retrieved by CLIP-based models on the MSCOCO dataset in response to various text queries. The images retrieved by MVAM-CLIP align more closely with the text queries, demonstrating robustness even with lengthy and intricate queries. For instance, the first example highlights that while the CLIP model retrieved an image of a "white fondant cake on pedestal", it did not fully match the detailed query descriptors, i.e. "white and green roses", "dark wire wide-mesh birdcage", and "a bird perched". In contrast, the top-1 image retrieved by MVAM-CLIP perfectly matches the query, showcasing MVAM's ability to encode detailed information into both images and texts. This capability significantly enhances the performance of the two-stream model, particularly in handling complex contents.

<i>Queries</i>	<i>Models</i>	<i>Top5 – Images</i>				
Two-tiered white fondant cake on pedestal with tiers separated by two rows of white and green roses covered with a dark wire wide-mesh birdcage top with a bird perched atop for a handle.	CLIP					
	MVAM-CLIP					
A computer screen has many colors, with a mouse and speakers next to it on the table.	CLIP					
	MVAM-CLIP					
A table with bowls of grains and fruit and a hand with a plate.	CLIP					
	MVAM-CLIP					

**Fig. 4.** The retrieved top5 images of CLIP and MVAM-CLIP. We lay out images according to the retrieval score and the ground-truth images are in green boxes. For long and complex text queries, the images retrieved by MVAM-CLIP are more suitable.



## 5 Conclusions

In this paper, we introduce the Multi-View Attention Method (MVAM) to enhance the representation quality of two-stream models for image-text matching. Unlike traditional approaches that encode an image or text into a single vector, MVAM encodes inputs according to diverse views, capturing more comprehensive information and preventing the omission of crucial details during the retrieval process. As a pluggable module, MVAM can be combined with any two-stream models. Experiment results on MSCOCO and Flickr30K show that with higher quality representations, our method can improve the matching performance by a significant margin. In addition, we conduct extensive experiments on studying the hyperparameters and loss functions of MVAM to search for the best model settings. The visualization of attention patterns across various views aids in understanding the focus of different views and demonstrates that our model effectively captures diverse information from both images and texts.

## 6 Acknowledgement

The authors wish to thank the anonymous reviewers for their helpful comments. This work was funded by the National Natural Science Foundation of China (NSFC) under Grants No. 62441229, and the Natural Science Foundation of Chongqing, China under Grants No. CSTB2022NSCQ-MSX1672.

## Bibliography

- [1] Anderson, P., He, X., Buehler, C., Teney, D., Johnson, M., Gould, S., Zhang, L.: Bottom-up and top-down attention for image captioning and visual question answering. In: Proceedings of the IEEE conference on computer vision and pattern recognition. pp. 6077–6086 (2018)
- [2] Avrahami, O., Hayes, T., Gafni, O., Gupta, S., Taigman, Y., Parikh, D., Lischinski, D., Fried, O., Yin, X.: Spatext: Spatio-textual representation for controllable image generation. In: Proceedings of the IEEE/CVF Conference on Computer Vision and Pattern Recognition. pp. 18370–18380 (2023)
- [3] Chen, Y.C., Li, L., Yu, L., El Kholy, A., Ahmed, F., Gan, Z., Cheng, Y., Liu, J.: Uniter: Learning universal image-text representations (2019)
- [4] Deng, J., Dong, W., Socher, R., Li, L.J., Li, K., Fei-Fei, L.: Imagenet: A large-scale hierarchical image database. In: 2009 IEEE conference on computer vision and pattern recognition. pp. 248–255. Ieee (2009)
- [5] Devlin, J., Chang, M.W., Lee, K., Toutanova, K.: Bert: Pre-training of deep bidirectional transformers for language understanding. arXiv preprint arXiv:1810.04805 (2018)
- [6] Devlin, J., Chang, M., Lee, K., Toutanova, K.: BERT: pre-training of deep bidirectional transformers for language understanding. CoRR **abs/1810.04805** (2018), <http://arxiv.org/abs/1810.04805>
- [7] Dosovitskiy, A., Beyer, L., Kolesnikov, A., Weissenborn, D., Zhai, X., Unterthiner, T., Dehghani, M., Minderer, M., Heigold, G., Gelly, S., et al.: An image is worth 16x16 words: Transformers for image recognition at scale. arXiv preprint arXiv:2010.11929 (2020)
- [8] Faghri, F., Fleet, D.J., Kiros, J.R., Fidler, S.: Vse++: Improving visual-semantic embeddings with hard negatives. arXiv preprint arXiv:1707.05612 (2017)
- [9] He, W., Jamonnak, S., Gou, L., Ren, L.: Clip-s4: Language-guided self-supervised semantic segmentation. In: Proceedings of the IEEE/CVF Conference on Computer Vision and Pattern Recognition. pp. 11207–11216 (2023)
- [10] Humeau, S., Shuster, K., Lachaux, M.A., Weston, J.: Poly-encoders: Transformer architectures and pre-training strategies for fast and accurate multi-sentence scoring. arXiv preprint arXiv:1905.01969 (2019)
- [11] Huo, Y., Zhang, M., Liu, G., Lu, H., Gao, Y., Yang, G., Wen, J., Zhang, H., Xu, B., Zheng, W., et al.: Wenlan: Bridging vision and language by large-scale multi-modal pre-training. arXiv preprint arXiv:2103.06561 (2021)
- [12] Jia, C., Yang, Y., Xia, Y., Chen, Y.T., Parekh, Z., Pham, H., Le, Q., Sung, Y.H., Li, Z., Duerig, T.: Scaling up visual and vision-language representation learning with noisy text supervision. In: International Conference on Machine Learning. pp. 4904–4916. PMLR (2021)

- [13] Karpathy, A., Fei-Fei, L.: Deep visual-semantic alignments for generating image descriptions. In: Proceedings of the IEEE conference on computer vision and pattern recognition. pp. 3128–3137 (2015)
- [14] Khattab, O., Zaharia, M.: Colbert: Efficient and effective passage search via contextualized late interaction over bert. In: Proceedings of the 43rd International ACM SIGIR conference on research and development in Information Retrieval. pp. 39–48 (2020)
- [15] Kim, G., Kwon, T., Ye, J.C.: Diffusionclip: Text-guided diffusion models for robust image manipulation. In: Proceedings of the IEEE/CVF conference on computer vision and pattern recognition. pp. 2426–2435 (2022)
- [16] Lee, K.H., Chen, X., Hua, G., Hu, H., He, X.: Stacked cross attention for image-text matching. In: Proceedings of the European Conference on Computer Vision (ECCV). pp. 201–216 (2018)
- [17] Li, G., Duan, N., Fang, Y., Gong, M., Jiang, D.: Unicoder-vl: A universal encoder for vision and language by cross-modal pre-training. In: Proceedings of the AAAI Conference on Artificial Intelligence. vol. 34, pp. 11336–11344 (2020)
- [18] Li, S., Bak, S., Carr, P., Wang, X.: Diversity regularized spatiotemporal attention for video-based person re-identification. In: Proceedings of the IEEE Conference on Computer Vision and Pattern Recognition. pp. 369–378 (2018)
- [19] Li, X., Yin, X., Li, C., Zhang, P., Hu, X., Zhang, L., Wang, L., Hu, H., Dong, L., Wei, F., et al.: Oscar: Object-semantics aligned pre-training for vision-language tasks. In: European Conference on Computer Vision. pp. 121–137. Springer (2020)
- [20] Li, Z., Fan, Z., Tou, H., Chen, J., Wei, Z., Huang, X.: Mvpnr: Multi-level semantic alignment for vision-language pre-training via multi-stage learning. Proceedings of the 30th ACM International Conference on Multimedia (2022), <https://api.semanticscholar.org/CorpusID:252222245>
- [21] Lin, T.Y., Maire, M., Belongie, S., Hays, J., Perona, P., Ramanan, D., Dollár, P., Zitnick, C.L.: Microsoft coco: Common objects in context. In: European conference on computer vision. pp. 740–755. Springer (2014)
- [22] Lin, Y., Chen, M., Wang, W., Wu, B., Li, K., Lin, B., Liu, H., He, X.: Clip is also an efficient segmenter: A text-driven approach for weakly supervised semantic segmentation. In: Proceedings of the IEEE/CVF Conference on Computer Vision and Pattern Recognition. pp. 15305–15314 (2023)
- [23] Lin, Z., Feng, M., Santos, C.N.d., Yu, M., Xiang, B., Zhou, B., Bengio, Y.: A structured self-attentive sentence embedding. arXiv preprint arXiv:1703.03130 (2017)
- [24] Lu, J., Batra, D., Parikh, D., Lee, S.: Vlbirt: Pretraining task-agnostic visiolinguistic representations for vision-and-language tasks. Advances in neural information processing systems **32** (2019)
- [25] Lu, X., Zhao, T., Lee, K.: Visualsparta: An embarrassingly simple approach to large-scale text-to-image search with weighted bag-of-words. arXiv preprint arXiv:2101.00265 (2021)

- [26] Luan, Y., Eisenstein, J., Toutanova, K., Collins, M.: Sparse, dense, and attentional representations for text retrieval. *Transactions of the Association for Computational Linguistics* **9**, 329–345 (2021)
- [27] Luo, H., Bao, J., Wu, Y., He, X., Li, T.: Segclip: Patch aggregation with learnable centers for open-vocabulary semantic segmentation. In: *International Conference on Machine Learning*. pp. 23033–23044. PMLR (2023)
- [28] Nichol, A., Dhariwal, P., Ramesh, A., Shyam, P., Mishkin, P., McGrew, B., Sutskever, I., Chen, M.: Glide: Towards photorealistic image generation and editing with text-guided diffusion models. *arXiv preprint arXiv:2112.10741* (2021)
- [29] Patashnik, O., Wu, Z., Shechtman, E., Cohen-Or, D., Lischinski, D.: Styleclip: Text-driven manipulation of stylegan imagery. In: *Proceedings of the IEEE/CVF international conference on computer vision*. pp. 2085–2094 (2021)
- [30] Qi, D., Su, L., Song, J., Cui, E., Bharti, T., Sacheti, A.: Imagebert: Cross-modal pre-training with large-scale weak-supervised image-text data. *arXiv preprint arXiv:2001.07966* (2020)
- [31] Radford, A., Kim, J.W., Hallacy, C., Ramesh, A., Goh, G., Agarwal, S., Sasstry, G., Aspell, A., Mishkin, P., Clark, J., et al.: Learning transferable visual models from natural language supervision. In: *International Conference on Machine Learning*. pp. 8748–8763. PMLR (2021)
- [32] Ramesh, A., Dhariwal, P., Nichol, A., Chu, C., Chen, M.: Hierarchical text-conditional image generation with clip latents. *arXiv preprint arXiv:2204.06125* **1**(2), 3 (2022)
- [33] Ren, S., He, K., Girshick, R., Sun, J.: Faster r-cnn: Towards real-time object detection with region proposal networks. *Advances in neural information processing systems* **28** (2015)
- [34] Song, Y., Soleymani, M.: Polysemous visual-semantic embedding for cross-modal retrieval. In: *Proceedings of the IEEE/CVF Conference on Computer Vision and Pattern Recognition*. pp. 1979–1988 (2019)
- [35] Sun, S., Chen, Y.C., Li, L., Wang, S., Fang, Y., Liu, J.: Lightningdot: Pre-training visual-semantic embeddings for real-time image-text retrieval. In: *Proceedings of the 2021 Conference of the North American Chapter of the Association for Computational Linguistics: Human Language Technologies*. pp. 982–997 (2021)
- [36] Wang, Z., Liu, W., He, Q., Wu, X., Yi, Z.: Clip-gen: Language-free training of a text-to-image generator with clip. *arXiv preprint arXiv:2203.00386* (2022)
- [37] Wang, Z., Liu, X., Li, H., Sheng, L., Yan, J., Wang, X., Shao, J.: Camp: Cross-modal adaptive message passing for text-image retrieval. In: *Proceedings of the IEEE/CVF International Conference on Computer Vision*. pp. 5764–5773 (2019)
- [38] Wu, B., Xu, C., Dai, X., Wan, A., Zhang, P., Yan, Z., Tomizuka, M., Gonzalez, J., Keutzer, K., Vajda, P.: Visual transformers: Token-based image representation and processing for computer vision (2020)

- [39] Young, P., Lai, A., Hodosh, M., Hockenmaier, J.: From image descriptions to visual denotations: New similarity metrics for semantic inference over event descriptions. *Transactions of the Association for Computational Linguistics* **2**, 67–78 (2014)
- [40] Zhang, Q., Lei, Z., Zhang, Z., Li, S.Z.: Context-aware attention network for image-text retrieval. In: *Proceedings of the IEEE/CVF Conference on Computer Vision and Pattern Recognition*. pp. 3536–3545 (2020)
- [41] Zhou, Z., Lei, Y., Zhang, B., Liu, L., Liu, Y.: Zegclip: Towards adapting clip for zero-shot semantic segmentation. In: *Proceedings of the IEEE/CVF Conference on Computer Vision and Pattern Recognition*. pp. 11175–11185 (2023)